

Unsupervised Concept Drift Detection from Deep Learning Representations in Real-time

Salvatore Greco
Politecnico di Torino
Turin, Italy
salvatore_greco@polito.it

Daniele Apiletti
Politecnico di Torino
Turin, Italy
daniele.apiletti@polito.it

Bartolomeo Vacchetti
Politecnico di Torino
Turin, Italy
bartolomeo.vacchetti@polito.it

Tania Cerquitelli
Politecnico di Torino
Turin, Italy
tania.cerquitelli@polito.it

ABSTRACT

Concept Drift is a phenomenon in which the underlying data distribution and statistical properties of a target domain change over time, leading to a degradation of the model’s performance. Consequently, models deployed in production require continuous monitoring through drift detection techniques. Most drift detection methods to date are supervised, i.e., based on ground-truth labels. However, true labels are usually not available in many real-world scenarios. Although recent efforts have been made to develop unsupervised methods, they often lack the required accuracy, have a complexity that makes real-time implementation in production environments difficult, or are unable to effectively characterize drift. To address these challenges, we propose DRIFTLens, an unsupervised real-time concept drift detection framework. It works on unstructured data by exploiting the distribution distances of deep learning representations. DRIFTLens can also provide drift characterization by analyzing each label separately. A comprehensive experimental evaluation is presented with multiple deep learning classifiers for text, image, and speech. Results show that (i) DRIFTLens performs better than previous methods in detecting drift in 11/13 use cases; (ii) it runs at least 5 times faster; (iii) its detected drift value is very coherent with the amount of drift (correlation ≥ 0.85); (iv) it is robust to parameter changes.

Artifact Availability:

The source code, data, and/or other artifacts have been made available at <https://github.com/grecoSalvatore/drift-lens>.

1 INTRODUCTION

The basic assumption of deep learning is that the training data mimics the real world. Nevertheless, deep learning models are typically trained and evaluated on static datasets. However, the world is dynamic, and the model learned during training may no longer be valid. The underlying data distribution and statistical properties of the target domain may change over time, leading to the models’ performance degradation (or decay) [41]. This phenomenon is called “concept drift”.

Concept drift and performance degradation can affect the reliability and robustness of deep learning models in real-world production applications [63]. Therefore, it is important to continuously monitor production models and detect concept/data drift at an early

stage [52]. This monitoring process should provide *early warnings* when a shift occurs and implement *adaptive measures* to maintain expected performance on newly processed data.

A large body of research has focused on detecting concept drift over time through *supervised* strategies. They typically rely on error rates or performance-based measures computed from actual labels [41]. However, in many real-world applications, the actual labels are not available for newly processed data.

A parallel research effort has been devoted to *unsupervised* strategies for detecting concept/data drift in data streams [22, 32, 53]. Most of them usually rely on distribution distances or divergence measures that are evaluated for each individual instance. Therefore, they are often computationally intensive and thus ineffective in detecting concept drift in the case of deep learning models working with unstructured data. In such scenarios, existing techniques are not suitable for detecting drift in (near) real-time. Moreover, many techniques show poor performance in detecting drift in high-dimensional data.

To overcome these limitations, this paper proposes DRIFTLens, an *unsupervised* drift detection framework for deep learning classifiers working with unstructured data. In designing DRIFTLens, we attempt to answer the following four research questions (RQs):

(RQ1) *To what extent can DRIFTLens detect drift of varying severity in deep learning classifiers for unstructured data in the absence of ground truth labels?*

(RQ2) *How can DRIFTLens be applied broadly and effectively across various data types, models, and classification tasks?*

(RQ3) *How efficient is DRIFTLens at detecting drift in near real-time?*

(RQ4) *To what extent can DRIFTLens accurately model and characterize the presence of drift over time?*

To this aim, the contribution of this paper is twofold:

(1) We propose DRIFTLens (§4), a new *unsupervised* drift detection framework able to detect *whether* and *when* drift occurs by computing the distribution distances of the deep learning embedding representations on unstructured data. DRIFTLens is able to perform *drift characterization* by determining which labels are most affected by the drift. Due to its low complexity, it can run in *real-time*.

(2) We perform a comprehensive evaluation of DRIFTLens for several deep learning models and datasets for text, image, and speech classification (§5). We found that: (i) DRIFTLens is very effective in

discriminating new data with and without drift. Overall, DRIFTLENS achieves better performance than previous techniques across 11/13 use cases. (ii) DRIFTLENS is extremely fast and enables real-time concept drift detection, as it can classify the presence of drift in less than 0.2 seconds independently of the data volumes, running at least 5 times faster than other detectors. (iii) The drift curve modeled by DRIFTLENS is highly correlated with the amount of drift present as it exhibits a correlation index ≥ 0.85 for the drift patterns evaluated. We also qualitatively show that the drifting trend is coherently represented by the drift curves, and that it is able to characterize drift by identifying the labels most affected by drift. (iv) DRIFTLENS is robust to its parameter settings.

Before discussing the methodology (§4) and the experimental evaluations (§5), we define the concept drift problem and the application scenario with the specific challenges we focus on in this paper (§2). Then, we highlight the limitations of previous work on concept drift detection in our setting (§3).

2 PROBLEM FORMULATION

Here, we formally define the concept drift problem (§2.1), we show the patterns in which drift can occur (§2.2), and we define the application scenario, challenges and desiderata in this study (§2.3).

2.1 Concept drift definition

Concept drift can be defined as a phenomenon in which the underlying data distribution and statistical properties of a target data domain change over time. The presence of drift can negatively affect the performance of predictive models over time. Various terms have been proposed to refer to “concept drift” [7], such as data drift, dataset shift, covariate shift, prior probability shift, and concept shift. Although each definition emphasizes a particular facet of the phenomenon, most works broadly refer to all subcategories under the term “concept drift”. Concept drift is defined as a change in the joint distribution between a time period $[0, t]$ and a time window $t + w$. Drift occurs at time window $t + w$ if:

$$P_{[0,t]}(X, y) \neq P_{t+w}(X, y) \quad (1)$$

Where X and y are the feature vectors and the target variable of each data instance (x_i, y_i) , and $P_t(X, y)$ is the joint probability. The time window $t + w$ can be defined as a time period or instant based on how the data stream is processed. The joint probability can be further decomposed as:

$$P_t(X, y) = P_t(y/X)P_t(X) = P_t(X/y)P_t(y) \quad (2)$$

Where, $P_t(X/y)$ is the class-conditional probability, $P_t(y/X)$ is the target labels posterior probability, $P_t(X)$ is the input data prior probability, and $P_t(y)$ is target labels prior probability. Therefore, in classification tasks, concept drift can occur as a change in any of these terms: (1) $P(X)$: A drift in the input data. The marginal probability of the input features X changes. This type of drift is also known as data drift, covariance drift, or virtual drift. (2) $P(y/X)$: The relationships or conditional probabilities of target labels given input features change, but the input features do not necessarily change. This is usually referred to as concept or real drift. (3) $P(y)$: A change in the output data. Therefore, the labels and their probabilities change. This type of drift is sometimes referred to as label drift.

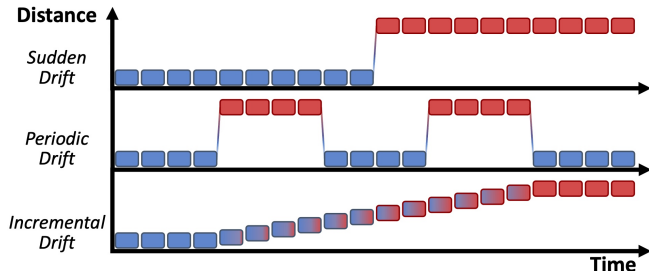


Figure 1: Drift patterns.

This work focuses on the detection of drift in production scenarios where no ground truth labels are available for new data. Therefore, drift has to be detected in an *unsupervised* way. Due to the lack of actual labels, the only possible drift to be considered is the change in the priority probability of the features $P(X)$ [32].

2.2 Drift patterns

Concept drift can occur in several patterns. Some examples are shown in Figure 1 and described below.

Sudden/abrupt change. Drift can occur suddenly if the distribution of new samples changes rapidly. A possible example of a sudden drift is a tweets topic classifier during the outbreak of the COVID-19 pandemic. At that point, the model was suddenly exposed to numerous text samples containing a new topic. Recognizing this scenario is crucial to initiate the retraining process and restore the classifier’s performance.

Recurrent change. Drift occurs repeatedly after the first observed event, with a seasonality unknown during training. For example, a topic or a sentiment classifier dealing with a new topic of interest, seasonal events, or cultural changes will lead to changes in the labels to be predicted. In an election year, the language and topics of discussion on social media platforms can change significantly, affecting the sentiment and context in which certain words or phrases are used. After the election, discussions return to a normal state, but during another significant event, such as a global sporting event like the Olympics, the state may change again. The classifier must adapt to these changes in order to perform well. However, as these changes occur repeatedly, it faces the challenge of the concept drifting in a cyclical pattern. It is important to recognize this scenario in order to possibly (i) retrain the classifiers to include examples of the new recurrent distribution or (ii) switch to another model that has been explicitly trained on the specific case.

Incremental change. The transition between concepts occurs smoothly and gradually over time. For instance, during image or object classification for autonomous vehicles, the model may encounter new vehicle types, such as scooters (i.e., Personal Light Electric Vehicles), which were not part of the original training data. Initially, these new vehicles appear only rarely and their occurrence is sporadic. Over time, however, they gradually become more commonplace and an integral part of the streetscape.

2.3 Application scenarios

We design DRIFTLENS so that it can be effectively exploited in a variety of application scenarios characterized by:

(1) *Unavailability of ground truth labels for new incoming data.* Many applications, such as sentiment analysis or topic detection on social media comments, deal with a data-intensive production to be classified through deep learning models. Most of them do not have actual labels available for newly processed samples. Therefore, both drift detection and adaptation must be made in an unsupervised way, as performed by DRIFTLENS.

(2) *High complexity and high-dimensional data.* Most applications deal with unstructured data, such as text, images, and speech. Detecting concept drift in unstructured data is even more complex than in structured data due to the high dimensionality (usually characterized by high data sparsity), the complexity of the inputs, and the lack of a fixed structure, such as columns. All those aspects can undermine the effectiveness and increase the complexity of drift detection techniques. Appropriate data modeling is required to detect data changes over time effectively. DRIFTLENS relies on the analysis of the internal representation generated by deep learning models to immediately detect concept drift in classifiers working with unstructured data.

In such a target scenario, the desiderata for the drift detection method are the following: (1) *Fast detection.* The drift detection technique should be able to detect drift as soon as possible and not only when drift occurs with high severity; (2) *Real-time detection.* The technique should have low complexity and be able to run in real-time; (3) *Drift characterization.* It should provide information on what type of drift occurs and evaluate the labels most affected by the data changes. DRIFTLENS addresses all the above desiderata.

3 RELATED WORKS

There has been a significant effort in the field of concept drift detection [2, 7, 22, 33, 41, 62]. Drift detection techniques can be categorized into two macro-categories based on the true labels availability assumption: (1) *supervised* and (2) *unsupervised*.

(1) **Supervised concept drift methods.** Most of the previous drift detection techniques are *supervised* [4, 5, 9, 18–20, 27, 28, 35, 37, 39, 43, 46, 55, 61, 66]. These methods typically rely on error rate-based measures or ensemble models to assess the performance degradation over time (e.g., accuracy decrease). However, these methods assume that true labels are available along with the new data or within a short period of time. In practice, the labels for new data are usually not available, and labeling them is very costly and time-consuming. This dependence on the availability of true labels is a major limitation of these techniques, which limits their applicability in real-world scenarios.

(2) **Unsupervised concept drift methods.** In contrast, *unsupervised* techniques do not require the availability of true labels [22, 32, 53, 65]. Our methodology falls into this category. As outlined by [32], unsupervised techniques can be further divided into: (2.i) *statistical-based*, (2.ii) *loss-based*, and (2.iii) *virtual classifier-based*.

(2.i) **Statistical-based methods.** Most of the unsupervised techniques rely on statistical tests or divergence metrics between two distributions [6, 10, 11, 13, 15, 26, 36, 45, 48, 60], usually between a reference and a new window. Our methodology belongs to this

Table 1: Symbols and notation.

Symbol	Description
$L; L $	Set of labels used to train the model; N° of labels.
$\phi(X)$	Encoder function that takes a set of inputs X and outputs the embedding E .
$d; d'$	Embedding dimensionality; Reduced embedding dimensionality.
\hat{y}	Vector of predicted labels.
$E; E'$	Embedding matrix; Reduced embedding matrix
$m; m_b; m_w$	N° of samples; N° of baseline samples; N° of window samples (window size).
$\mu; \mu_b; \mu_w$	Mean vector; Baseline mean vector; Window mean vector.
$\Sigma; \Sigma_b; \Sigma_w$	Covariance matrix; Baseline covariance matrix; Window covariance matrix.
$m_w; m_b$	Window size; Size of the reference set.
n_{th}	Number of randomly sampled windows to estimate the threshold.
$T; T_{\alpha}$	Threshold value; Threshold sensitivity.

category. These techniques are independent of the type of data and models and do not require external models or resources. Most of these techniques use every single sample in the reference and new window to calculate the distances. Therefore, they do not scale with the number of samples and the dimensionality of the inputs. This can affect both their runtime and drift prediction performance.

(2.ii) **Loss-based methods.** These techniques exploit machine learning model loss functions to evaluate the similarity of newly arrived data points with previous ones [34, 42, 56, 67]. Usually, they rely on auto-encoders or are used in conjunction with supervised drift detectors. In the first case, these methods are widely used but are difficult to transfer to other types of distributions. In the second case, they rely on the assumption that there is a correlation between the increase in model losses and the concept drift, as shown in [31]. Moreover, their implementation varies depending on the data type, typically being less effective for texts or speech compared to images.

(2.iii) **Virtual classifier-based methods.** Also these techniques, such as [23, 30, 38], implement classifiers to detect drift but in a different way. The general idea is to divide data into two sets, before and after a certain moment in time. If the classifier achieves an accuracy higher than random in classifying samples into the two classes, it implies divergent data properties between the two class distributions, which means that there is drift. The limitation of these approaches lies in their need to train and maintain a new model to detect drift.

Drift adaptation and incremental learning. Some supervised works are related to incremental learning for drift detection and adaptation [21]. However, in unsupervised settings, the adaptation to drift is much more challenging due to the lack of annotated samples [32]. The drift adaptation problem is out of the scope of this paper. Instead, we focus on the drift detection problem only.

This paper presents a new unsupervised statistical-based drift detection technique, namely DRIFTLENS. The preliminary idea was presented in [24]. DRIFTLENS differs from previous work in three key aspects. Firstly, like other statistical-based methods, it is completely unsupervised. Thus, it does not require any external model to detect drift, unlike supervised, loss-based, and virtual classifier methods. Secondly, it exploits statistical distances that better scale with data dimensionality than other statistical-based methods, thereby enabling efficient real-time drift detection in large data volumes. Thirdly, DRIFTLENS is able to better characterize drift by identifying each drifting label.

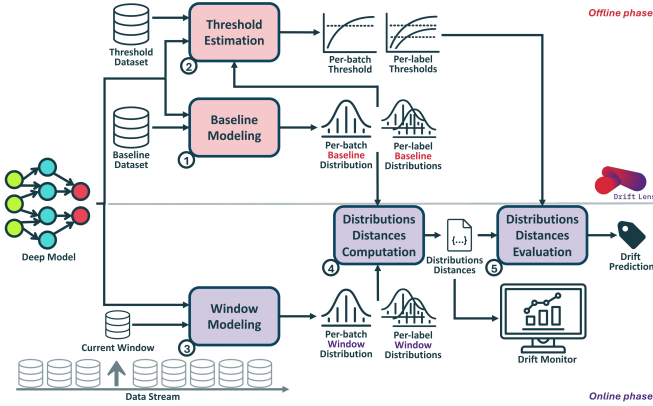


Figure 2: DRIFTLens framework. It comprises an *offline* and an *online* phases. In the *offline* phase, it estimates the reference distributions and distance thresholds from historical (training) data. The distributions are modeled as multivariate normal and are computed: (i) for the entire batch (*per-batch*), and (ii) conditioned on the predicted label (*per-label*). In the *online* phase, it analyzes data streams in fixed windows, comparing new and reference distributions, and using thresholds to identify drift, visualized through a drift trend monitor.

4 DRIFTLens

DRIFTLens is an *unsupervised* drift detection technique based on distribution distances within the embeddings, i.e., the internal dense representations generated by deep learning models. It is specifically designed to deal with unstructured data and uses the nuanced patterns and relationships represented in the embeddings to detect data shifts or changes over time. The methodology includes an *offline* and an *online* phases, as shown in Figure 2. In the *offline* phase, DRIFTLens estimates the *reference distributions* and *threshold values* from the historical (e.g., training) dataset. The reference distributions, called *baseline*, represent the distribution of features (i.e., embedding) of the concepts that the model has learned during the training phase. They, therefore, represent the absence of drift. In the *online* phase, the new data stream is processed in windows of fixed size. Firstly, the distributions of the new data windows are estimated. Secondly, the distribution distances are computed with respect to the reference distributions. If the distance exceeds the threshold, the presence of drift is predicted.

We first present the data modeling (§4.1) and the distribution distance used (§4.2), as they are performed similarly in both phases. Then, we describe the *offline* (§4.3) and *online* (§4.4) phases. Table 1 reports a list of symbols used to describe the methodology.

4.1 Data modeling

The goal of data modeling is to estimate the distribution of a batch of data. Instead of using the raw input data, we exploit the internal representation that the deep learning model generates when processing a batch of data (i.e., the embeddings). Figure 3 summarizes the main steps of the data modeling performed by DRIFTLens. It estimates (i) the embedding distribution of the entire batch independent of the predicted class labels (*per-batch*) and (ii) the embedding

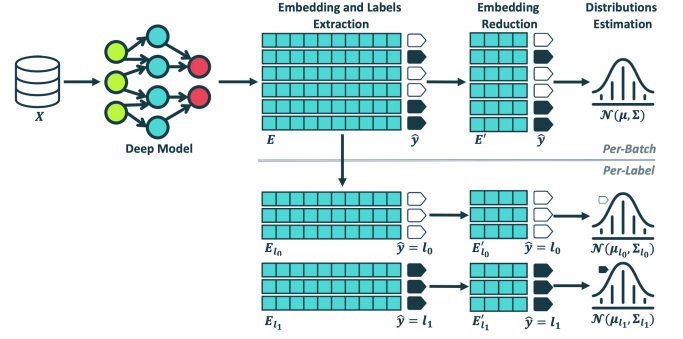


Figure 3: DRIFTLens data modeling. This process inputs a deep learning model and a set of data, and estimates the multivariate normal embedding distributions. It extracts embeddings from the model, enriches them with labels, reduces the embedding dimensionality, and estimates the *per-batch* distribution by computing the mean vector μ and covariance matrix Σ . It further estimates label-specific distributions by grouping embeddings by label, reducing the dimensionality, and computing the *per-label* μ_l and Σ_l , $\forall l \in L$.

distributions for each predicted class separately (*per-label*). The *per-batch* models the entire set of embedding vectors as a multivariate normal distribution. For the *per-label*, $|L|$ normal distributions are estimated instead, where $|L|$ is the number of labels on which the model was trained. In our framework, we assume that the embeddings are distributed as a multivariate normal distribution. Although this is usually a strong assumption for the raw input features, it may be a good approximation when applied to the features in the embedding space. This is because the dense features in the embedding space, especially in the last layers, have simpler relationships [8] and can be better approximated as a multivariate normal distribution.

Consider a deep learning classifier capable of distinguishing between a set of class labels L . The classifier consists of an encoder part $\phi(X)$ that maps the sparse and complex representations of the raw input data to a dense and simpler latent representation by applying several nonlinear transformations using some learned weights W . The encoder is usually followed by one or more fully connected neural network layers to predict a class label based on the latent embedding representation.

In data modeling, a dataset X (i.e., the entire baseline or a new window) is fed into the deep learning model to extract the corresponding embedding matrix $E = \phi(X) \in \mathbb{R}^{m \times d}$ and the vector of predicted labels $\hat{y} \in \mathbb{R}^m$, where m is the number of samples in the set and d is the dimensionality of the extracted embedding layer. For deep learning classifiers, the dimensionality of the embedding space is usually large (i.e., in the range of thousands). Since we model the embedding as a multivariate normal distribution, we need to compute the mean vector μ and the covariance matrix Σ over the set of vectors. However, the covariance matrix Σ requires at least d linearly independent vectors (i.e., inputs) to be full rank. Otherwise, it will contain complex numbers that affect the computation of the distribution distance (see §4.2). This problem is particularly pronounced when estimating an arbitrary multivariate

normal distribution for each label, as we need d linearly independent vectors predicted with each label. Although this is usually not a problem when modeling the baseline as it is computed over the entire historical dataset (e.g., the training set), in the online phase d linearly independent vectors are needed to estimate the distribution per batch, and $d \times |L|$ linearly independent vectors are needed to estimate the per-label distributions in each data stream window. Therefore, the fixed size used to divide the data stream into windows must be very large. To solve this problem, DRIFTLens performs a dimensionality reduction of the embedding by applying a principal component analysis (PCA) step.

$$E' = \text{PCA}(E) \quad (3)$$

This leads to a reduced embedding matrix $E' \in \mathbb{R}^{m \times d'}$, where $0 < d' \leq d$ is a user-defined parameter that determines the number of principal components for the entire batch. Dimensionality reduction is also performed separately for each embedding matrix, depending on the predicted label.

$$E'_l = \text{PCA}(E_l), \forall l \in L \quad (4)$$

Where $E_l \in \mathbb{R}^{m_l \times d'_l}$ are the embedding vectors associated with the inputs predicted with the label l , and $0 < d'_l \leq d$ is a user-defined parameter that specifies the number of principal components for each label. Note that d' and d'_l can be set to different values. For the per-batch, d' can possibly be set to $d' = \min(m_w, d)$, where m_w is the window size used in the online phase and d is the embedding dimensionality. In our experiments (see §5), we always set $d = 150$. Instead, d'_l depends on the window size, the dimensionality of the embedding, and the number of labels. A reasonable suggestion for a balanced data stream is to set its value close to $d'_l = \min(m_w/|L|, d)$.

Note that the PCA models are fitted and used in the offline phase to reduce the dimensionality of the embedding. In the online phase, the PCA models that were fitted in the offline phase are used instead to reduce the embedding of the new data.

Once performed the dimensionality reduction, the reduced embedding matrices E' and E'_l are used to estimate the multivariate normal distribution of the *per-batch* (equation 5), and the $|L|$ multivariate normal distribution of each predicted label (equation 6).

$$P(\phi(x); W) \sim \mathcal{N}(\mu, \Sigma) \quad (5)$$

$$P(\phi(x) | \hat{y} = l; W) \sim \mathcal{N}(\mu_l, \Sigma_l), \forall l \in L \quad (6)$$

Where $\mu \in \mathbb{R}^{d'}$ and $\Sigma \in \mathbb{R}^{d' \times d'}$ are the mean vector and the covariance matrix of the *per-batch* multivariate normal distribution, and each $\mu_l \in \mathbb{R}^{d'}$ and $\Sigma_l \in \mathbb{R}^{d' \times d'}$ represents the *per-label* multivariate normal distribution of each label $l \in L$, separately. The multivariate normal distributions are straightforward and fast to estimate because they can be fully characterized by the mean vector and the covariance matrix. The main advantage of estimating the distributions as multivariate normal distributions is that they can be represented with dimensionality d' , regardless of the number of samples in the reference and new windows. This allows the method to scale well even with large amounts of data and enables the detection of drifts in real-time regardless of the data volumes.

4.2 Distribution distance

DRIFTLens uses the Frechét distance [17] to calculate the distance between two multivariate normal distributions. The Frechét distance, also known as the Wasserstein-2 distance [64], has been widely used in deep learning to measure the distances between the distributions of models' features, but in very different scenarios [29]. DRIFTLens uses the Frechét distance to measure the distances between the embedding distributions of a baseline (reference distributions) and the new windows in the data stream, and we call it *Frechét Drift Distance (FDD)*.

Starting from a reference multivariate normal distribution (e.g., the baseline distribution) b characterized by a mean vector μ_b and a covariance matrix Σ_b , and the multivariate normal distribution of the new data window w , characterized by μ_w and Σ_w , the *FDD* is computed as follows:

$$FDD(b, w) = \|\mu_b - \mu_w\|_2^2 + \text{Tr}\left(\Sigma_b + \Sigma_w - 2\sqrt{\Sigma_b \Sigma_w}\right) \quad (7)$$

Where $FDD(b, w) \in \mathbb{R}$ in $[0, \infty]$. The higher the *FDD*, the greater the distance, and the more likely the drift. *FDD* takes into account changes in the mean (i.e., center) and the diagonal elements of the covariance (i.e., spread) between the two distributions. The former results from the L2 norm of the difference between the mean vectors $\|\mu_b - \mu_w\|_2^2$. The latter by considering $\text{Tr}(\Sigma_b + \Sigma_w - 2\sqrt{\Sigma_b \Sigma_w})$. This last term can be considered as the generalization of the squared difference between the standard deviations in one-dimensional space. Therefore, the *FDD* score can potentially be useful to identify more subtle types of drift that affect not only the center of the distributions but also the spread.

DRIFTLens computes a single *per-batch* distance by computing the *FDD* score between the baseline (μ_b, Σ_b) and the new window (μ_w, Σ_w) *per-batch* distributions, and $|L|$ *per-label* distances by computing the distance of the distributions ($\mu_{b,l}, \Sigma_{b,l}$) and ($\mu_{w,l}, \Sigma_{w,l}$) for each label $l \in L$ separately.

4.3 Offline phase

In the *offline* phase (steps 1 and 2 in Figure 2), DRIFTLens estimates (i) the probability distribution of a reference dataset that represents what the model learned during training, and (ii) distance thresholds to distinguish between normal and abnormal (i.e., possible drift) distances. The *offline* phase is run once, and its results are permanently stored on disk for later use during the *online* phase.

4.3.1 Baseline estimation. The baseline estimation consists of performing the data modeling (§4.1) on the baseline dataset and permanently storing the estimated distributions and the PCA models on disk. Specifically, given a baseline dataset X_b , containing m_b samples, the entire baseline dataset X_b is fed into the deep learning model to extract the embedding vectors $E_b = \phi(X_b)$ and estimate the vector of predicted labels \hat{y}_b . Then, the *per-batch* PCA is fitted over the entire set of vectors, and $|L|$ different PCAs are fitted, grouping the embedding vectors according to the predicted labels. The embedding vectors are then reduced both for the *per-batch*, to obtain the reduced embedding matrix E'_b , and for the *per-label*, to obtain the $|L|$ reduced embedding matrices $E'_{b,l}$. The embedding

matrices are then used to estimate the baseline *per-batch* and *per-label* multivariate normal distributions. The *per-batch* distribution is fully characterized by the baseline *per-batch* mean vector μ_b and the covariance matrix Σ_b , which are obtained by calculating the mean and covariance over the entire set of reduced embedding vectors in the baseline dataset. The *per-label* distributions are obtained by computing the $|L|$ mean vectors $\mu_{b,l}$ and the covariance matrices $\Sigma_{b,l}$ on the reduced embedding vectors, grouped by predicted labels. Note that regardless of the dimensionality of the reference set m_b (i.e., the baseline), the offline phase estimates distributions characterized by vectors of size d' . Thus, when predicting the drift for new windows, it is not influenced by the reference set m_b .

4.3.2 Threshold estimation. The threshold estimation aims to identify the maximum possible distance (*FDD*) that a given window without drift can reach. To this end, DRIFTLens takes in input the threshold dataset X_{th} , the window size m_w (equal to the one that will be used in the online phase), the baseline, and a parameter n_{th} defining the number of windows to be randomly sampled from the threshold dataset. The n_{th} parameter should be as large as possible to better estimate the larger distance in data considered without drift. In our experiments (see §5.1), we empirically set $n_{th} = 10000$. However, we found that varying this parameter does not significantly impact the framework (see §5.5).

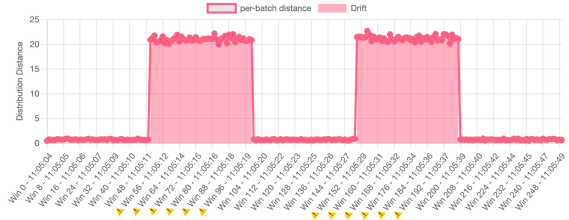
Specifically, DRIFTLens randomly sample n_{th} windows from the threshold dataset X_{th} , each one containing m_w inputs. For each window, it performs the data modeling phase and computes the *per-batch* and *per-label* distribution distances with respect to the baseline distributions. Therefore, n_{th} distribution distances for the entire batch and each label are computed. Finally, the distribution distances are sorted in descending order. The first element contains the maximum distance a window of data considered without drift can have with respect to the baseline. Thus, distances that exceed this value are potential warnings of drift. However, there are potentially outlier distances due to the large number of randomly sampled windows. Therefore, DRIFTLens provides a parameter to define the threshold sensitivity $T_\alpha \in [0, 1]$. This parameter removes the $T_\alpha\%$ left tail of the sorted distances (in descending order) to remove outliers. The final thresholds T and T_l are set to the maximum distance after removing the $T_\alpha\%$ of the more considerable distances. Therefore, the higher the value of T_α , the lower the values of the thresholds, and the higher the sensitivity to possible drift and false alarm. In our experiments (see §5.1), we use $T_\alpha = 0.01$ as a default threshold sensitivity value because we want to take the maximum possible distance by just removing the outliers (top 1%).

4.3.3 Choice of the reference dataset. The reference set must be historical data representing what the model learned during training. Ideally, the entire training set can be used as the baseline, and the test set or a number of windows from the real data stream, assumed they could represent distributions without drift, for the threshold dataset. In our experiments, we use the training set for the baseline and the test set for the threshold estimation (see §5.1).

4.4 Online phase

In the *online* phase (steps 3, 4, and 5 in Figure 2), DRIFTLens processes the new data stream into fixed-size windows. The window

Per-Batch Drift Detection



Per-Label Drift Detection

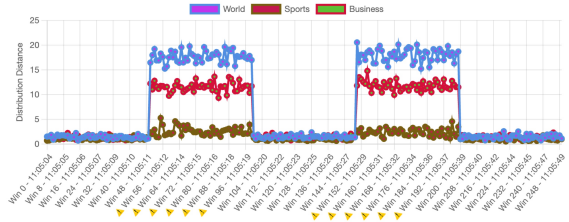


Figure 4: DRIFTLens monitor example. It shows the *per-batch* and each *per-label* distribution distances (*FDD*) over time.

size is defined by the parameter m_w . Given a new data window X_w containing m_w new samples, the data modeling is processed by (i) extracting the embedding $E_w \in \mathbb{R}^{m_w \times d}$ and predicted labels $\hat{y}_w \in \mathbb{R}^{m_w}$, (ii) performing the embedding dimensionality reduction to obtain $E'_w \in \mathbb{R}^{m_w \times d'}$, and (iii) estimating the *per-batch* and *per-label* multivariate normal distributions. The PCA models fitted during the offline phase are used in this step. The *per-batch* multivariate normal distribution is obtained by computing the mean vector $\mu_w \in \mathbb{R}^{d'}$ and the covariance matrix $\Sigma_w \in \mathbb{R}^{d' \times d'}$ over the entire set of embeddings in the window. For the *per-label*, a multivariate normal distribution for each distinct label is obtained by selecting the embedding vectors predicted with such label and computing the mean and covariance on that subset, obtaining the $|L|$ multivariate normal distributions characterized by $\mu_{w,l} \in \mathbb{R}^{d'}$ and $\Sigma_{w,l} \in \mathbb{R}^{d' \times d'}$. Finally, the *per-batch* and the *per-label* *FDD* distances between the window and baseline distributions are computed (equation 7). If the *per-batch* and/or the *per-label* distribution distances exceed the threshold values, drift is predicted. The former is essential to detect if the entire window is affected by drift. The latter characterizes drift and identifies the most impacted labels.

4.4.1 Drift monitoring over time. The same process is repeated for each window. Once DRIFTLens processes a new window, the *FDD* distribution distances are added to the drift monitor. The drift monitor shows in two separate charts the *per-batch* and *per-label* distribution distances. A warning symbol is added to the plot when a given distance exceeds the corresponding threshold. The drift monitor provides valuable insights to understand (i) when and whether drift occurs, (ii) the severity of the drift and the patterns, and (iii) what are the labels the most affected by drift.

Figure 4 shows an example of the drift monitor.¹ The above chart shows the *per-batch*, while the bottom shows the *per-label* distribution distances for all the windows. The *x-axis* reports the

¹Generated with the DRIFTLens web tool [25].

timestamps and the window identifiers, while the distribution distances (FDD) are in the y -axis. When drift is detected (i.e., the distribution distance in a given window is above the threshold), the area under the curve is filled, and a warning is displayed in the x -tick of the charts. In this case, the monitor shows that drift occurs for the first time after 50 windows with high severity, and then reoccurs intermittently with non-drifted windows with a periodic pattern. The label *World* is the most affected by drift, followed by *Business*. Instead, the label *Sports* is negligibly impacted.

5 EVALUATION

To evaluate the ability of DRIFTLens in detecting drift across various deep learning classifiers for text, image, and speech data (introduced in §5.1), we evaluate the drift detection performance (§5.2) and the execution time (§5.3) in comparison with state-of-the-art drift detectors. Then, we evaluate its ability to accurately characterize drift (§5.4), and analyze its sensitivity to parameter setting (§5.5).

5.1 Experimental settings

To demonstrate the effectiveness of DRIFTLens in detecting different types of drift in different scenarios, we conduct experiments with several use cases, which are summarized in Table 2. Use cases are categorized into groups based on the dataset used, the task chosen, and the way the drift is simulated. Within each group, different deep learning models are considered and evaluated. By evaluating DRIFTLens on a variety of experiments, we aim to demonstrate the broad applicability and generalizability of the proposed framework.

Deep learning classifiers. We perform experiments with several deep learning models suitable for NLP (BERT² [14], DistilBERT³ [50], and RoBERTa⁴ [40]), computer vision (VGG16⁵ [54] and Visual Transformer⁶ [16]), and speech (Wav2Vec⁷ [51]) classification tasks.

Datasets. Since we focus on working with unstructured data, we have selected several well-known datasets. In the NLP domain, we trained models for topic detection by using the Ag News [68] and 20 Newsgroups [44] datasets. In the computer vision domain, we used the Intel Image [49] and STL-10 [12] datasets for image classification. In the speech domain, we used the Common Voice [3] dataset to train a model for classifying the gender of speakers.

Drift simulation. To investigate the applicability of DRIFTLens to different application scenarios, we simulated different drift sources. In the use cases from 1 to 5 in Table 2, drift is simulated by introducing a new unknown class label. Specifically, we used two subsets of the dataset to train (fine-tune) and test the models. A third part of the dataset is kept away to generate the windows in the data stream (i.e., to simulate new, unseen data with a similar distribution to the training). Drift is simulated by removing one of the class labels during training and presenting these examples in the data stream windows. In use case 3, the same dataset is used as in use case 2, but the nature of drift is more subtle, as only a subset of a class is used to simulate drift by exploiting the hierarchical categorization of the

dataset. In contrast, in use cases 6 and 7 in Table 2, we simulate drift by changing the properties of the input features. In use case 6, drift is simulated by blurring the input images. Specifically, we introduce a Gaussian blur with radius 4 on a circular patch that covers an area of $D\%$ of the entire image, where $D\%$ corresponds to the percentage of drift we want to insert. For use case 7, drift is simulated instead by presenting the model with speech samples in English accents other than those used for training (i.e., Australian, Canadian, and Scottish).

Embedding extraction. For the BERT, DistilBERT, RoBERTa, and Visual Transformer (Vi-T) models, we extract the embedding of the [CLS] token from the last hidden layer (embedding dimensionality $d = 768$). For VGG16, we extract and flatten the last convolutional layer ($d = 4608$). For Wav2Vec, we extract and average all the representations of the last transformers’ hidden layer ($d = 768$).

Windows generation. When generating windows of the data streams, we use samples with or without drift that the model has never seen during the training or testing phase. The dimensionality of the data split is specified in the last column of Table 2. When creating a window without drift, we randomly select a balanced sample by class label from the new data without drift. These examples represent new data, never seen by the model, but with the same distribution as the training data. When generating windows containing $D\%$ of drift, we randomly select $D\%$ of the window size (m_w) from the drifted samples, while the remaining $(100 - D)\%$ are balanced samples from the new unseen samples without drift. Use case 6 is the only exception where a percentage $D\%$ of the pixels in all images are blurred. Windows are sampled with replacement due to dimensionality constraints (i.e., some samples may belong to more than one window).

DriftLens configuration. The following are the default experimental parameters of DRIFTLens. The *offline* phase exploits the entire training and test sets, the former for the baseline modeling, and the latter for the threshold estimation. The dimensionality of the training and test set for each use case is indicated in Table 2. We set $d' = 150$ as the number of principal components used to reduce the *per-batch* embedding, except for use case 7 where we set $d' = 25$ to have full rank matrices. The number of windows in the threshold estimation $n_{th} = 10k$, and its sensitivity is $T_\alpha = 0.01$. The window size is kept fixed in both the *offline* and *online* phases.

Comparison techniques. We compare DRIFTLens with four unsupervised statistical-based drift detection techniques from previous work: Maximum Mean Discrepancy⁸ (MMD) [26], Kolmogorov-Smirnov⁹ (KS) [15], Least-Squares Density Difference¹⁰ (LSD) [10], and Cramér-von Mises¹¹ (CVM) drift detection techniques. We use the implementation provided by the Alibi Detect library [57]. We keep the default parameters configuration of each technique. The *p-value* to discriminate between drifted and non-drifted distributions is set to 0.05 as the default. All the techniques require a reference dataset. Due to complexity reasons, the reference dataset is obtained by randomly sampling a subset of the training with $m_b = 5000$ balanced samples, except for the 20 Newsgroup dataset,

²<https://huggingface.co/google-bert/bert-base-uncased>

³<https://huggingface.co/distilbert/distilbert-base-uncased>

⁴<https://huggingface.co/facebookAI/roberta-base>

⁵<https://keras.io/api/applications/vgg/>

⁶<https://huggingface.co/google/vit-base-patch16-224>

⁷<https://huggingface.co/facebook/wav2vec2-base>

⁸<https://docs.seldon.io/projects/alibi-detect/en/stable/cd/methods/mmdrift.html>

⁹<https://docs.seldon.io/projects/alibi-detect/en/stable/cd/methods/ksdrift.html>

¹⁰<https://docs.seldon.io/projects/alibi-detect/en/stable/cd/methods/lssdrift.html>

¹¹<https://docs.seldon.io/projects/alibi-detect/en/stable/cd/methods/cvmdrift.html>

Table 2: Overview of the experimental use cases. Use cases are partitioned into groups based on the dataset and task. The training labels, the way the drift is simulated, and the split of the dataset are given in the description for each group. Within each group, different deep learning models are considered, and the corresponding F1 scores obtained on the test set are given.

Data Type	Dataset	Task	Use Case	Models	F1	Description
Text	Ag News	Topic Detection	1.1	BERT	0.98	Training Labels: <i>World, Business, and Sport</i> Drift: Simulated with one new class label: <i>Science/Tech</i> Dataset Split: 59,480 train - 5,700 test - 30,520 without drift data stream - 31,900 drifted dataset stream
			1.2	DistilBERT	0.97	
			1.3	RoBERTa	0.98	
Text	20 Newsgroups	Topic Detection	2.1	BERT	0.88	Training Labels: <i>Technology, Sale-Ads, Politics, Religion, Science</i> (5 macro-labels) Drift: Simulated with one new class: <i>Recreation</i> (1 macro-label) Dataset Split: 5,080 train - 3,387 test - 5,560 without drift data stream - 3,655 drifted dataset stream
			2.2	DistilBERT	0.87	
			2.3	RoBERTa	0.88	
Text	20 Newsgroups	Topic Detection	3	BERT	0.87	Training Labels: Training on 6 labels: 5 macro-labels: <i>Technology, Sale-Ads, Politics, Religion, Science</i> and a subset of the macro-label <i>Recreation: baseball and hockey</i> Drift: Simulated with another subset of the macro-label <i>Recreation: motorcycles and autos</i> Dataset Split: 5,744 train - 3,829 test - 6,304 without drift data stream - 1,805 drifted dataset stream
Image	Intel Image	Image Classification	4.1	Vi-T	0.90	Training Labels: <i>Forest, Glacier, Mountain, Building, Street</i> Drift: Simulated with one new class label: <i>Sea</i> Dataset Split: 6,000 train - 4,000 test - 4,256 without drift data stream - 2,780 drifted dataset stream
			4.2	VGG16	0.89	
Image	STL-10	Image Classification	5.1	Vi-T	0.96	Training Labels: <i>Airplane, Bird, Car, Cat, Deer, Dog, Horse, Monkey, Sheep</i> Drift: Simulated with one new class label: <i>Truck</i> Dataset Split: 5,850 train - 2,925 test - 2,925 without drift data stream - 1,300 drifted dataset stream
			5.2	VGG16	0.82	
Image	STL-10	Image Classification	6	Vi-T	0.90	Training Labels: <i>Airplane, Bird, Car, Cat, Deer, Dog, Horse, Monkey, Sheep, Truck</i> Drift: Simulated by introducing blur in the images within the same labels Dataset Split: 6,500 train - 3,250 test - 3,250 without drift data stream - 3,250 drifted dataset stream
Speech	Common Voice	Gender Identification	7	Wav2Vec	0.91	Training Labels: <i>Male, Female</i> (US and UK accent) Drift: Introduced with speeches from same labels but different accent (Australian, Canadian, Scottish) Dataset Split: 70,578 train - 9,951 test - 29,556 without drift data stream - 42,697 drifted dataset stream

where we used $m_b \approx 1700$ for use case 2, and $m_b \approx 2050$ for use case 3, to make them balanced. Similarly to our framework, we use the embedding vectors as input.

5.2 Drift detection performance evaluation

This evaluation aims to determine the effectiveness of DRIFTLENS in detecting windows containing drifted samples of varying severity (to answer RQ1 in §1). We treat the drift detection problem as a binary classification task. The task is to predict whether a window of new samples contains drift. We perform the evaluation for different models, data types, and tasks to assess the general applicability of DRIFTLENS (to answer RQ2 in §1).

Evaluation metrics. We use the *accuracy* as an evaluation measure for the drift prediction performance with different degrees of severity $D\% \in \{0\%, 5\%, 10\%, 15\%, 20\%\}$. If a window contains any percentage of drifted examples $D\%$, the ground truth is set to 1; otherwise, it is set to 0. Data windows without drift (i.e., $D = 0\%$) are used to measure type I errors (i.e., no drift, but the technique has detected one; false alarm). For each drift percentage $D\%$, use case, and window size m_w , we randomly draw 100 windows. Each window contains m_w samples, with $D\%$ of the samples drawn from the drift dataset. The accuracy is calculated over the 100 windows, repeated 5 times, and then averaged. At each run, the DRIFTLENS’ threshold is re-estimated and the reference set of the other detectors is re-sampled. However, since the predictions of drifted and non-drifted windows are closely related, if a technique always predicts drift, it should be considered unreliable. Therefore, we first calculate the average accuracy in detecting drift:

$$\bar{A}_{\text{drift}} = (A_{5\%} + A_{10\%} + A_{15\%} + A_{20\%})/4 \quad (8)$$

Then, we introduce a *Harmonic Drift Detection* (H_{DD}) mean between the mean accuracy for non-drifted windows, and the mean accuracy

of the drifted windows \bar{A}_{drift} , as follows:

$$H_{DD} = \frac{2}{\frac{1}{A_{0\%}} + \frac{1}{\bar{A}_{\text{drift}}}} \quad (9)$$

The H_{DD} is a real number in the range $[0, 1]$ that measures the overall quality of the drift detector in distinguishing between windows with and without drift. The H_{DD} disfavors techniques that always predict the presence or absence of drift (i.e., $A_{0\%} = 0$ or $\bar{A}_{\text{drift}} = 0$). In such cases, $H_{DD} = 0$.

Results. Table 3 and Table 4 show the drift prediction accuracy, broken down by severity, and the H_{DD} score for all the techniques and use cases. Table 3 uses larger data windows than Table 4 as the datasets contain more samples. For each use case, each drift detector, and each window size, the following values are reported: (i) the mean accuracy by drift percentage, and (ii) the overall harmonic drift detection mean H_{DD} .

For larger data volumes (Table 3), DRIFTLENS achieves better drift prediction performance over all the experimental use cases independently of the data type and window size. For use cases 1.1, 1.2, and 1.3, it is particularly effective in detecting drift, achieving an $H_{DD} \geq 0.93$, except for use case 1.3 with window size 500 where the H_{DD} is slightly slower. Interestingly, DRIFTLENS is the only effective technique for the speech task (use case 7). The better performance with a high volume of data is probable due to the FDD distance, which is more reliable with large data volumes when estimating the reference distributions and the threshold values.

For smaller data volume (Table 4), overall is the most effective technique. However, for some use cases (e.g., 5.2 and 6), other techniques such as MDD or LSDD achieve better H_{DD} scores. Surprisingly, all detectors are able to identify the drift simulated with blur (use case 6). However, some of them (KS and CVM) exhibit a large number of false positives, especially for larger window sizes. In addition, DRIFTLENS is the only technique that consistently achieves

Table 3: Drift detection performance evaluation for larger data volume. For each drift detector and window size ($m_w \in \{500, 1000, 2000\}$) are reported: i) the accuracy separately for each drift percentage ($D\% \in \{0\%, 5\%, 10\%, 15\%, 20\%\}$), and the harmonic drift detection mean H_{DD} . Each accuracy is computed over 100 windows and averaged repeating 5 runs. The best-performing detector based on the H_{DD} for each use case and window size is in bold.

Use Case	Drift Detector	Data Stream Window Size m_w																	
		$m_w = 500$						$m_w = 1000$						$m_w = 2000$					
		Drift Percentage $D\%$					H_{DD}	Drift Percentage $D\%$					H_{DD}	Drift Percentage $D\%$					H_{DD}
0%	5%	10%	15%	20%	0%	5%		10%	15%	20%	0%	5%		10%	15%	20%			
1.1	MMD	1.00	0.00	0.15	0.96	1.00	<i>0.69</i>	1.00	0.00	0.73	1.00	1.00	<i>0.81</i>	1.00	0.00	1.00	1.00	1.00	<i>0.86</i>
	KS	1.00	0.00	0.14	0.95	1.00	<i>0.69</i>	1.00	0.00	0.83	1.00	1.00	<i>0.97</i>	1.00	0.24	1.00	1.00	1.00	<i>0.90</i>
	LSDD	1.00	0.00	0.08	0.87	1.00	<i>0.66</i>	1.00	0.00	0.37	1.00	1.00	<i>0.74</i>	1.00	0.03	1.00	1.00	1.00	<i>0.86</i>
	CVM	1.00	0.00	0.15	0.96	1.00	<i>0.69</i>	1.00	0.03	0.84	1.00	1.00	<i>0.84</i>	1.00	0.31	1.00	1.00	1.00	<i>0.91</i>
	DRIFTLens	0.99	0.83	1.00	1.00	1.00	0.97	1.00	0.98	1.00	1.00	1.00	1.00	0.97	1.00	1.00	1.00	1.00	0.98
1.2	MMD	1.00	0.00	0.06	0.83	1.00	<i>0.64</i>	1.00	0.00	0.73	1.00	1.00	<i>0.81</i>	1.00	0.00	1.00	1.00	1.00	<i>0.86</i>
	KS	1.00	0.01	0.21	0.76	1.00	<i>0.66</i>	1.00	0.02	0.67	1.00	1.00	<i>0.80</i>	1.00	0.04	1.00	1.00	1.00	<i>0.86</i>
	LSDD	1.00	0.00	0.03	0.51	0.98	<i>0.55</i>	1.00	0.00	0.32	1.00	1.00	<i>0.73</i>	1.00	0.00	0.99	1.00	1.00	<i>0.86</i>
	CVM	1.00	0.00	0.08	0.86	1.00	<i>0.65</i>	0.99	0.02	0.80	1.00	1.00	<i>0.82</i>	1.00	0.09	1.00	1.00	1.00	<i>0.87</i>
	DRIFTLens	0.99	0.71	1.00	1.00	1.00	0.96	0.99	0.98	1.00	1.00	1.00	0.99	0.99	1.00	1.00	1.00	1.00	0.99
1.3	MMD	1.00	0.00	0.14	0.95	1.00	<i>0.69</i>	1.00	0.00	0.97	1.00	1.00	<i>0.85</i>	1.00	0.00	1.00	1.00	1.00	<i>0.86</i>
	KS	1.00	0.00	0.17	0.78	1.00	<i>0.66</i>	1.00	0.01	0.75	1.00	1.00	<i>0.82</i>	1.00	0.02	1.00	1.00	1.00	<i>0.86</i>
	LSDD	1.00	0.00	0.12	0.94	1.00	<i>0.68</i>	1.00	0.00	0.82	1.00	1.00	<i>0.83</i>	1.00	0.00	1.00	1.00	1.00	<i>0.86</i>
	CVM	1.00	0.01	0.06	0.86	1.00	<i>0.65</i>	1.00	0.01	0.84	1.00	1.00	<i>0.83</i>	1.00	0.02	1.00	1.00	1.00	<i>0.86</i>
	DRIFTLens	1.00	0.09	0.98	1.00	1.00	0.87	1.00	0.47	1.00	1.00	1.00	0.93	1.00	0.96	1.00	1.00	1.00	1.00
7	MMD	0.15	0.94	0.99	1.00	1.00	<i>0.26</i>	0.00	1.00	1.00	1.00	1.00	<i>0.00</i>	0.00	1.00	1.00	1.00	1.00	<i>0.00</i>
	KS	0.15	0.90	0.96	0.99	1.00	<i>0.26</i>	0.00	1.00	1.00	1.00	1.00	<i>0.00</i>	0.00	1.00	1.00	1.00	1.00	<i>0.00</i>
	LSDD	0.05	0.98	0.99	1.00	1.00	<i>0.10</i>	0.00	1.00	1.00	1.00	1.00	<i>0.00</i>	0.00	1.00	1.00	1.00	1.00	<i>0.00</i>
	CVM	0.08	0.94	0.98	1.00	1.00	<i>0.15</i>	0.00	1.00	1.00	1.00	1.00	<i>0.00</i>	0.00	1.00	1.00	1.00	1.00	<i>0.00</i>
	DRIFTLens	0.97	0.07	0.17	0.27	0.42	0.38	0.93	0.19	0.38	0.58	0.85	0.65	0.84	0.42	0.75	0.95	0.99	0.81

effective performance across all the use cases and window sizes ($H_{DD} \geq 0.60$), except for use case 5.2 with window size 250. In contrast, the other techniques always present some use cases for which they are totally unreliable ($H_{DD} = 0$).

In summary, DRIFTLens is highly effective in detecting windows containing drift (answering RQ1 in §1). It is also the most reliable and generally applicable technique across models, datasets, and data volumes, as it is the only detector that achieves good performance over all the experimental use cases (answering RQ2 in §1).

5.3 Complexity evaluation

This evaluation aims to ascertain the effectiveness of DRIFTLens to perform near real-time drift detection. To this end, we compare the running time of the drift detectors by varying the reference and data stream windows sizes, and the embedding dimensionality.

Evaluation metrics. We measure the mean running time in seconds to provide the drift prediction for each data window, given the embeddings already extracted. The experiments are executed on an Apple M1 MacBook Pro 13 2020 with 16GB of RAM.

Results. Figure 5 shows the running time in seconds on a logarithmic scale of each drift detector by varying (a) the reference window size m_b , (b) the data stream window size m_w , and (c) the embedding dimensionality d . One dimension at a time is varied, and the others are held fixed at the following values: window size $m_w = 1000$, embedding dimensionality $d = 1000$, and reference window size $m_b = 5000$. DRIFTLens outperforms all the evaluated techniques in terms of running time, running at least 5 times faster. Moreover, its execution time increases almost negligibly as the number of variables analyzed increases, while the other techniques are highly affected by the window sizes and embedding dimensionality.

Figure 6 shows DRIFTLens' running time when dealing with a large volume of data. In this case, the reference window is increased up to 500k samples, and the data stream window is up to 10k. The other drift detectors do not work with such dimensionalities. When varying the reference window size (m_b), the data stream window size is kept fixed to $m_w = 5000$. Instead, when varying the data stream window size (m_w), the reference window size is kept fixed to $m_b = 500k$. Figure 6-(a) confirms that the running time of DRIFTLens is almost independent of the size of the reference window, as only the distributions are loaded in the online phase (mean vector and covariance matrix with dimensionality d'). Additionally, Figure 6-(b) shows that the running time increases almost negligibly as the window size increases. It can, therefore, be used for real-time drift detection even on data streams with high throughput. Notably, the running time is always lower to 0.2 seconds.

In summary, DRIFTLens is the fastest detector in terms of running time. It can detect drift in near real-time independently of the amount of data in the reference set and in the data stream, as well as the embedding dimensionality (answering RQ3 in §1).

5.4 Drift curve evaluation

This evaluation aims to measure the ability of DRIFTLens to coherently represent and characterize the drift curve.

Evaluation metrics. We use the Spearman correlation coefficient [1] to measure the correlation between the *per-batch* (FDD) distances over time and the curve of injected drift. The Spearman correlation evaluates the monotonic relationship (i.e., when two variables tend to move in the same direction at a constant rate). Thus, it is more suitable for the non-linearities present in the evaluated patterns (e.g., sudden and periodic). The coefficient ranges

Table 4: Drift detection performance evaluation for *smaller* data volume. For each drift detector and window size ($m_w \in \{250, 500, 1000\}$) are reported: i) the accuracy separately for each drift percentage ($D\% \in \{0\%, 5\%, 10\%, 15\%, 20\%\}$) and the harmonic drift detection mean H_{DD} . Each accuracy is computed over 100 windows and averaged repeating 5 runs. The best-performing detector based on the H_{DD} for each use case and window size is in bold.

Use Case	Drift Detector	Data Stream Window Size m_w																	
		$m_w = 250$					$m_w = 500$					$m_w = 1000$							
		Drift Percentage $D\%$					Drift Percentage $D\%$					Drift Percentage $D\%$							
0%	5%	10%	15%	20%	H_{DD}	0%	5%	10%	15%	20%	H_{DD}	0%	5%	10%	15%	20%	H_{DD}		
2.1	MMD	0.83	0.33	0.74	0.98	1.00	0.80	0.06	1.00	1.00	1.00	1.00	0.11	0.00	1.00	1.00	1.00	1.00	0.00
	KS	0.00	1.00	1.00	1.00	1.00	0.00	0.00	1.00	1.00	1.00	1.00	0.00	0.00	1.00	1.00	1.00	1.00	0.00
	LSDD	1.00	0.01	0.04	0.19	0.48	0.31	0.98	0.14	0.41	0.76	0.96	0.72	0.61	0.65	0.93	1.00	1.00	0.72
	CVM	0.00	1.00	1.00	1.00	1.00	0.00	0.00	1.00	1.00	1.00	1.00	0.00	0.00	1.00	1.00	1.00	1.00	0.00
	DRIFTLens	0.92	0.28	0.68	0.96	1.00	0.81	0.89	0.42	0.92	1.00	1.00	0.86	0.84	0.78	1.00	1.00	1.00	0.89
2.2	MMD	1.00	0.01	0.08	0.61	0.98	0.59	0.95	0.12	0.63	1.00	1.00	0.80	0.56	0.72	1.00	1.00	1.00	0.70
	KS	0.42	0.68	0.89	1.00	1.00	0.57	0.01	0.99	1.00	1.00	1.00	0.02	0.00	1.00	1.00	1.00	1.00	0.00
	LSDD	1.00	0.00	0.01	0.05	0.25	0.14	1.00	0.01	0.06	0.35	0.83	0.48	0.98	0.03	0.33	0.92	0.99	0.72
	CVM	0.31	0.74	0.90	1.00	1.00	0.46	0.00	1.00	1.00	1.00	1.00	0.00	0.00	1.00	1.00	1.00	1.00	0.00
	DRIFTLens	1.00	0.15	0.72	0.99	1.00	0.83	1.00	0.23	0.95	1.00	1.00	0.89	1.00	0.40	1.00	1.00	1.00	0.92
2.3	MMD	1.00	0.00	0.06	0.40	0.91	0.51	0.96	0.22	0.78	1.00	1.00	0.84	0.37	0.95	1.00	1.00	1.00	0.54
	KS	0.33	0.84	0.06	0.40	0.91	0.41	0.00	1.00	1.00	1.00	1.00	0.00	0.00	1.00	1.00	1.00	1.00	0.00
	LSDD	1.00	0.00	0.00	0.03	0.09	0.06	1.00	0.00	0.03	0.17	0.51	0.30	0.97	0.09	0.36	0.86	1.00	0.72
	CVM	0.26	0.87	0.98	1.00	1.00	0.41	0.00	1.00	1.00	1.00	1.00	0.00	0.00	1.00	1.00	1.00	1.00	0.00
	DRIFTLens	0.98	0.08	0.26	0.57	0.88	0.61	0.98	0.07	0.34	0.82	0.99	0.71	0.99	0.07	0.53	0.98	1.00	0.78
3	MMD	1.00	0.00	0.04	0.59	0.98	0.57	0.99	0.08	0.76	1.00	1.00	0.83	0.48	0.89	1.00	1.00	1.00	0.61
	KS	0.01	1.00	1.00	1.00	1.00	0.02	0.00	1.00	1.00	1.00	1.00	0.00	0.00	1.00	1.00	1.00	1.00	0.00
	LSDD	1.00	0.00	0.00	0.03	0.35	0.17	1.00	0.00	0.02	0.55	0.99	0.56	1.00	0.01	0.41	1.00	1.00	0.75
	CVM	0.00	1.00	1.00	1.00	1.00	0.00	0.00	1.00	1.00	1.00	1.00	0.00	0.00	1.00	1.00	1.00	1.00	0.00
	DRIFTLens	0.97	0.21	0.65	0.96	1.00	0.82	0.98	0.35	0.94	1.00	1.00	0.89	0.98	0.63	1.00	1.00	1.00	0.94
4.1	MMD	1.00	0.00	0.00	0.43	0.99	0.52	1.00	0.00	0.18	1.00	1.00	0.71	1.00	0.00	0.97	1.00	1.00	0.85
	KS	1.00	0.00	0.02	0.39	0.97	0.51	1.00	0.00	0.18	0.99	1.00	0.70	1.00	0.01	0.92	1.00	1.00	0.85
	LSDD	1.00	0.00	0.00	0.20	0.73	0.38	1.00	0.00	0.05	0.86	1.00	0.65	1.00	0.00	0.57	1.00	1.00	0.78
	CVM	1.00	0.00	0.02	0.45	0.99	0.54	1.00	0.00	0.25	1.00	1.00	0.72	1.00	0.01	0.98	1.00	1.00	0.86
	DRIFTLens	1.00	0.01	0.30	1.00	1.00	0.73	1.00	0.00	0.35	1.00	1.00	0.74	1.00	0.00	0.50	1.00	1.00	0.77
4.2	MMD	1.00	0.00	0.09	0.67	0.99	0.61	1.00	0.01	0.47	0.99	1.00	0.76	1.00	0.05	0.98	1.00	1.00	0.86
	KS	1.00	0.00	0.00	0.02	0.32	0.16	1.00	0.00	0.00	0.31	0.97	0.47	1.00	0.00	0.15	1.00	1.00	0.70
	LSDD	0.98	0.05	0.05	0.07	0.10	0.13	0.98	0.04	0.07	0.13	0.22	0.21	0.96	0.03	0.11	0.20	0.47	0.33
	CVM	0.00	1.00	1.00	1.00	1.00	0.00	0.00	1.00	1.00	1.00	1.00	0.00	0.00	1.00	1.00	1.00	1.00	0.00
	DRIFTLens	0.95	0.06	0.17	0.61	0.94	0.61	0.94	0.14	0.66	0.99	1.00	0.80	0.93	0.31	0.98	1.00	1.00	0.87
5.1	MMD	1.00	0.00	0.06	1.00	1.00	0.68	1.00	0.00	1.00	1.00	1.00	0.86	1.00	0.07	1.00	1.00	1.00	0.87
	KS	0.97	0.11	0.33	0.99	1.00	0.75	0.83	0.54	0.97	1.00	1.00	0.85	0.37	0.98	1.00	1.00	1.00	0.54
	LSDD	1.00	0.00	0.01	1.00	1.00	0.67	1.00	0.00	0.97	1.00	1.00	0.85	1.00	0.03	1.00	1.00	1.00	0.86
	CVM	0.95	0.14	0.39	0.99	1.00	0.76	0.75	0.62	0.97	1.00	1.00	0.82	0.26	0.99	1.00	1.00	1.00	0.41
	DRIFTLens	0.96	0.82	1.00	1.00	1.00	0.96	0.96	1.00	1.00	1.00	1.00	0.98	0.97	1.00	1.00	1.00	1.00	0.99
5.2	MMD	0.98	0.03	0.25	0.93	1.00	0.71	0.99	0.04	0.76	1.00	1.00	0.82	0.99	0.03	1.00	1.00	1.00	0.86
	KS	1.00	0.00	0.01	0.11	0.57	0.29	1.00	0.00	0.05	0.70	1.00	0.61	1.00	0.01	0.32	1.00	1.00	0.74
	LSDD	0.95	0.04	0.05	0.20	0.63	0.63	0.99	0.03	0.05	0.72	1.00	0.62	0.95	0.06	0.43	1.00	1.00	0.75
	CVM	0.00	1.00	1.00	1.00	1.00	0.00	0.00	1.00	1.00	1.00	1.00	0.00	0.00	1.00	1.00	1.00	1.00	0.00
	DRIFTLens	0.98	0.00	0.05	0.20	0.60	0.35	1.00	0.04	0.12	0.77	1.00	0.65	1.00	0.07	0.70	1.00	1.00	0.82
6	MMD	1.00	1.00	1.00	1.00	1.00	1.00	1.00	1.00	1.00	1.00	1.00	1.00	1.00	1.00	1.00	1.00	1.00	1.00
	KS	0.93	1.00	1.00	1.00	1.00	0.96	0.65	1.00	1.00	1.00	1.00	0.79	0.11	1.00	1.00	1.00	1.00	0.20
	LSDD	1.00	0.00	0.03	0.24	0.77	0.41	1.00	1.00	1.00	1.00	1.00	1.00	1.00	1.00	1.00	1.00	1.00	1.00
	CVM	0.92	1.00	1.00	1.00	1.00	0.96	0.61	1.00	1.00	1.00	1.00	0.76	0.08	1.00	1.00	1.00	1.00	0.15
	DRIFTLens	0.95	1.00	1.00	1.00	1.00	0.97	0.93	1.00	1.00	1.00	1.00	0.96	0.92	1.00	1.00	1.00	1.00	0.96

from -1 to +1, where +1 (-1) indicates a perfect positive (negative) monotonic relationship, and 0 indicates no monotonic relationship. The curve of injected drift is composed of 0 in the windows without the presence of drift, and the percentage of drift ($D\%$) in the windows containing some drift. We also qualitatively evaluate the *per-batch* and *per-label* drift curves for three drift patterns.

Results. Table 5 reports the mean and the standard deviation of the Spearman correlation coefficient computed over all the experimental use cases. The data streams are generated by randomly sampling 100 windows containing 1000 samples each. In the sudden pattern, drift comes after 50 windows and is constant with a percentage of $D\% = 40\%$. In the incremental pattern, drift comes after 50 windows with a percentage of $D\% = 20\%$ and increases by $\Delta D\% = 1\%$ after

each window. In the periodic pattern, 20 windows without drift and 20 windows containing $D\% = 40\%$ of drift reoccur periodically. The experiments are repeated 5 times and averaged.

Table 5 reveals that the *per-batch* (FDD) distance is highly correlated with the generated drift curves. The Spearman correlation coefficient is always ≥ 0.85 for the three considered drift patterns. Notably, for the incremental pattern, it is almost 1. These results quantitatively demonstrate the ability of DRIFTLens to correctly characterize the drift trend over time.

Figure 7 and Figure 8 show two examples of DRIFTLens monitors obtained generating the sudden (a), incremental (b), and periodic (c) drift patterns, using the previously described settings. For both use cases, the *per-batch* and *per-label* drift curves are coherent with the

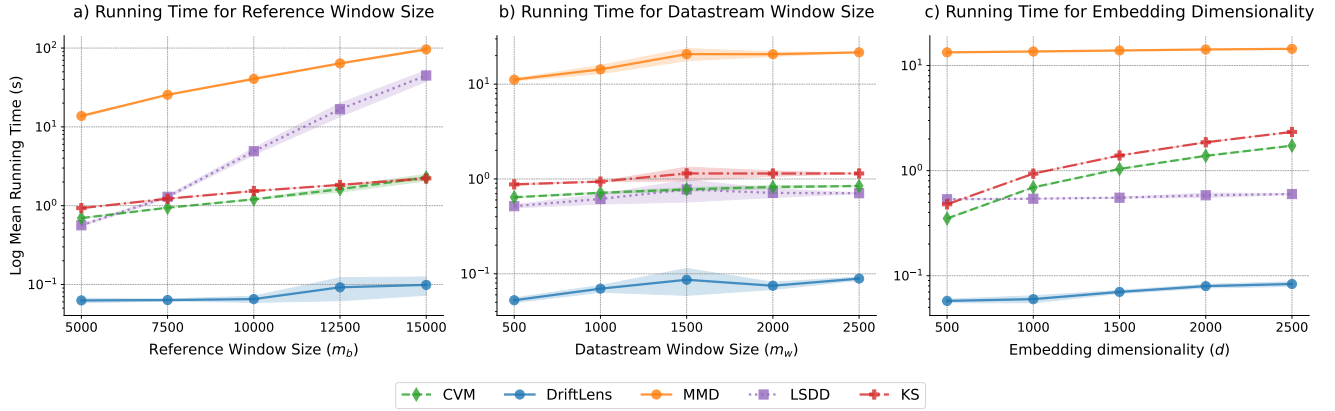


Figure 5: Running time comparison. For each drift detector, the mean and the standard deviation of the running time in seconds to process a new window are reported by varying (a) the reference window size, (b) the size of the data stream window, and (c) the embedding dimensionality, while keeping the other sizes fixed. The fixed values are: reference window size $m_b = 5000$, window size $m_w = 1000$, and embedding dimensionality $d = 1000$. Mean and std. are computed over 5 runs. Time is on a logarithmic scale.

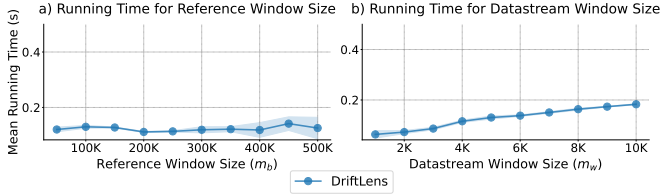


Figure 6: DRIFTLENS mean running time in seconds as the reference m_b (a) and data stream m_w (b) window sizes change.

Table 5: Drift patterns evaluation. Spearman correlation between the amount of drift and the *per-batch* distribution distance (*FDD*) for different drift patterns and use cases.

	Drift Pattern		
	<i>Sudden</i>	<i>Incremental</i>	<i>Recurrent</i>
<i>Corr.</i>	$0.875 \pm .02$	$0.993 \pm .01$	$0.849 \pm .00$

generated pattern. In use case 1.1 (Figure 7), the labels *World* (red) and *Business* (green) are the most impacted by drift. This probably happens because most of the examples of the new injected class (i.e., *Science/Technology*) are classified with those labels. Similarly, in use case 4.1 (Figure 8), the most impacted labels are *Mountain* (green) and *Street* (orange). These plots show that the *per-label* (*FDD*) curves provide valuable insights about the drift characterization by showing which labels are the most impacted by drift.

In summary, the trend of the drift curve generated by DRIFTLENS is highly coherent with the amount of drift present, and thanks to the *per-label* analysis, it is able to provide useful insights for characterizing the drift (answering RQ4 in §1).

Table 6: Parameters sensitivity.

Use Case	Parameter	Drift Percentage $D\%$					H_{DD}
		0%	5%	10%	15%	20%	
Number of sampled windows for threshold estimation n_{th}							
1.1	$n_{th} = 1k$	1.00	1.00	1.00	1.00	1.00	1.00
	$n_{th} = 5k$	0.99	0.99	1.00	1.00	1.00	0.99
	$n_{th} \in \{100, 10k, 25k\}$	0.99	1.00	1.00	1.00	1.00	0.99
5.1	$n_{th} = 1k$	0.93	1.00	1.00	1.00	1.00	0.96
	$n_{th} \in \{5k, 10k, 15k, 20k\}$	0.96	1.00	1.00	1.00	1.00	0.98
Threshold sensitivity T_α							
1.1	$T_\alpha = 0.00$	1.00	0.82	1.00	1.00	1.00	0.97
	$T_\alpha = 0.01$	0.99	1.00	1.00	1.00	1.00	0.99
	$T_\alpha = 0.05$	0.95	1.00	1.00	1.00	1.00	0.97
	$T_\alpha = 0.10$	0.90	1.00	1.00	1.00	1.00	0.95
	$T_\alpha = 0.25$	0.75	1.00	1.00	1.00	1.00	0.86
	5.1	$T_\alpha = 0.00$	1.00	1.00	1.00	1.00	1.00
$T_\alpha = 0.01$		0.97	1.00	1.00	1.00	1.00	0.98
$T_\alpha = 0.05$		0.90	1.00	1.00	1.00	1.00	0.95
$T_\alpha = 0.10$		0.83	1.00	1.00	1.00	1.00	0.91
$T_\alpha = 0.25$		0.68	1.00	1.00	1.00	1.00	0.81
Number of principal components d'							
1.1	$d' = 50$	0.97	1.00	1.00	1.00	1.00	0.98
	$d' = 100$	0.99	0.99	1.00	1.00	1.00	0.99
	$d' \in \{150, 200, 250\}$	0.99	1.00	1.00	1.00	1.00	0.99
5.1	$d' = 50$	0.95	1.00	1.00	1.00	1.00	0.97
	$d' \in \{100, 150, 200, 250\}$	0.97	1.00	1.00	1.00	1.00	0.98

5.5 Parameters sensitivity evaluation

This evaluation aims to determine the robustness and sensitivity of DRIFTLENS to its parameters. To this end, we evaluate its performance in drift prediction by varying the values of the following parameters: (i) the number of randomly sampled windows to estimate the threshold n_{th} , (ii) the threshold sensitivity parameter T_α , and (iii) the number of principal components used to reduce the dimensionality of the embedding d' .

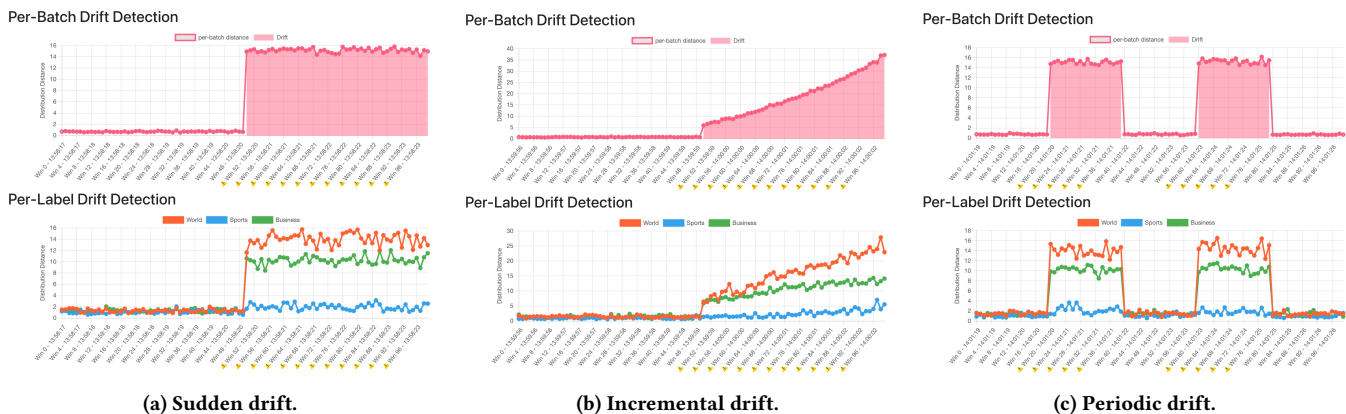


Figure 7: Drift patterns qualitative evaluation use case 1.1.

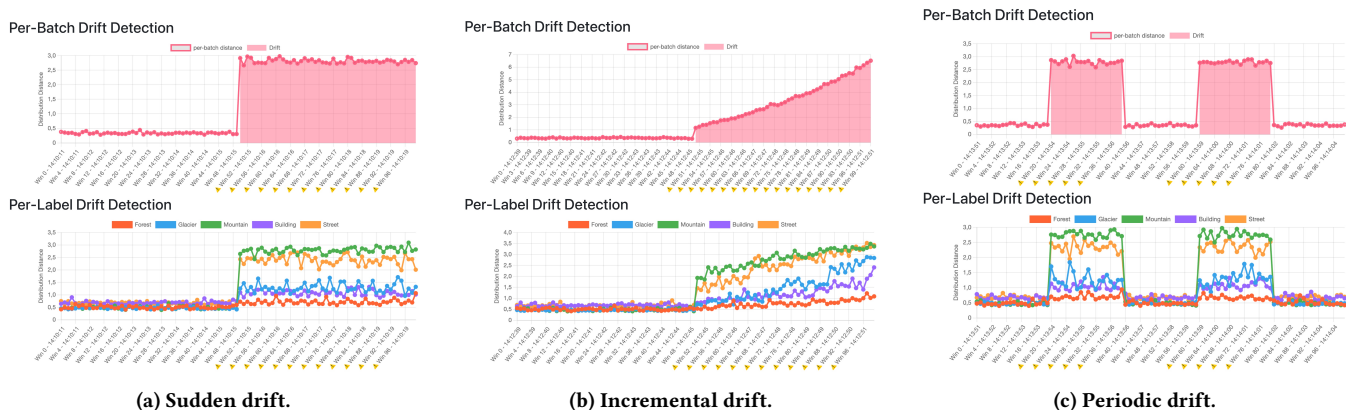


Figure 8: Drift patterns qualitative evaluation use case 4.1.

Evaluation metrics. We measure the *accuracy* in predicting drift with different severity levels and the H_{DD} .

Results. Table 6 reports the accuracy and H_{DD} by varying one parameter at a time while keeping the others fixed. The default fixed values are underlined and set to the following values: $n_{th} = 10k$, $T_\alpha = 0.01$, and $d' = 150$. The experiments are repeated 5 times and averaged for use cases 1.1 and 5.1.

The results indicate that varying the parameter values has minimal impact on performance, with a maximum reduction of 0.03. The only exception is the threshold sensitivity T_α value. As this parameter increases, DRIFTLens reduces its estimated threshold values, resulting in an increase in false positives—normal windows incorrectly identified as drift. This leads to reduced accuracy, especially when there is no actual drift ($D\% = 0\%$). However, we can conclude that the performance of DRIFTLens is not significantly affected by the choice of parameters, except for the threshold sensitivity.

6 CONCLUSION

This paper presents DRIFTLens, an *unsupervised* drift detection framework for deep learning models and unstructured data. It can be used to continuously monitor deep learning production models

to detect *whether* and *when* drift occurs to increase their reliability and robustness in real-world production applications. Our experiments show that DRIFTLens is effective in detecting drift and also more efficient than state-of-the-art techniques. Thanks to its fast execution time, it enables the detection of concept drift in real-time. Moreover, it correctly represents the drift trend over time and characterizes each drifting label.

Limitations. DRIFTLens uses the Fréchet distance to compute the distances between the baseline and the new window distributions (i.e., FDD). It can, therefore, inherit some of its limitations: (1) *Noise and selection bias with small datasets.* For small datasets, the FDD can potentially be affected by noise and selection bias in the distance calculation. However, we show empirically that DRIFTLens performs well even with smaller reference data and window sizes. (2) *Limited number of statistics used.* The FDD score uses a limited number of statistics in the distance calculation (i.e., mean and covariance). Therefore, it may not cover all aspects of the distributions. For example, while it covers the first two moments of the distribution, it does not take into account other moments (e.g., skewness and kurtosis). (3) *Distance score range.* The FDD score calculates distances in the range of $[0, \infty]$. However, it would be

more interpretable in the range of $[0, 1]$. In the future, we can overcome this limitation by expressing the distance in a relative value with respect to the threshold. Finally, (4) we always addressed drift in windows with balanced label distributions in our evaluations. However, in many scenarios, this hypothesis might not hold.

In **future work**, we would like to (i) integrate explainability techniques based on the embedding representations [58, 59] or concept-based explanations [47] to propose an explainable concept drift detection tool, (ii) address the problem of drift adaptation in unsupervised or supervised environments with limited labels; (iii) test the drift detectors in scenarios with unbalanced data distributions; (iii) extend the proposed approach to tasks other than classification; (iv) detect concept drift on multimodal models.

REFERENCES

- [1] 2008. *Spearman Rank Correlation Coefficient*. Springer New York, New York, NY, 502–505. https://doi.org/10.1007/978-0-387-32833-1_379
- [2] Jan Niklas Adams, Cameron Pitsch, Tobias Broekhoff, and Wil M. P. van der Aalst. 2023. An Experimental Evaluation of Process Concept Drift Detection. *Proc. VLDB Endow.* 16, 8 (apr 2023), 1856–1869. <https://doi.org/10.14778/3594512.3594517>
- [3] Rosana Ardila, Megan Branson, Kelly Davis, Michael Kohler, Josh Meyer, Michael Henretty, Reuben Morais, Lindsay Saunders, Francis Tyers, and Gregor Weber. 2020. Common Voice: A Massively-Multilingual Speech Corpus. In *Proceedings of the Twelfth Language Resources and Evaluation Conference*. European Language Resources Association, Marseille, France, 4218–4222. <https://aclanthology.org/2020.lrec-1.520>
- [4] Shruti Arora, Rinkle Rani, and Nitin Saxena. 2023. SETL: a transfer learning based dynamic ensemble classifier for concept drift detection in streaming data. *Cluster Computing* (Oct. 2023). <https://doi.org/10.1007/s10586-023-04149-w>
- [5] M Baena-Garcia, J Del Campo-Ávila, R Fidalgo, A Bifet, R Gavaldá, and R Morales-Bueno. 2006. Early drift detection method. *Fourth international workshop on knowledge discovery from data streams 6* (2006), 77–86.
- [6] Sulaimon A. Bashir, Andrei Petrovski, and Daniel Doolan. 2016. UDetect: Unsupervised Concept Change Detection for Mobile Activity Recognition. In *Proceedings of the 14th International Conference on Advances in Mobile Computing and Multi Media* (Singapore, Singapore) (*MoMM '16*). Association for Computing Machinery, New York, NY, USA, 20–27. <https://doi.org/10.1145/3007120.3007144>
- [7] Firas Bayram, Bestoun S. Ahmed, and Andreas Kassler. 2022. From Concept Drift to Model Degradation: An Overview on Performance-Aware Drift Detectors. *Know.-Based Syst.* 245, C (jun 2022). <https://doi.org/10.1016/j.knosys.2022.108632>
- [8] Yoshua Bengio, Aaron Courville, and Pascal Vincent. 2013. Representation Learning: A Review and New Perspectives. *IEEE Transactions on Pattern Analysis and Machine Intelligence* 35, 8 (2013), 1798–1828. <https://doi.org/10.1109/TPAMI.2013.50>
- [9] Albert Bifet and Ricard Gavaldá. 2007. Learning from time-changing data with adaptive windowing. In *Proceedings of the 2007 SIAM international conference on data mining*. SIAM, 443–448.
- [10] Li Bu, Cesare Alippi, and Dongbin Zhao. 2018. A pdf-Free Change Detection Test Based on Density Difference Estimation. *IEEE Transactions on Neural Networks and Learning Systems* 29, 2 (2018), 324–334. <https://doi.org/10.1109/TNNLS.2016.2619909>
- [11] Tania Cerquitelli, Stefano Proto, Francesco Ventura, Daniele Apiletti, and Elena Baralis. 2019. Towards a Real-Time Unsupervised Estimation of Predictive Model Degradation. In *Proceedings of Real-Time Business Intelligence and Analytics* (Los Angeles, CA, USA) (*BIRTE 2019*). Association for Computing Machinery. <https://doi.org/10.1145/3350489.3350494>
- [12] Adam Coates, Andrew Ng, and Honglak Lee. 2011. An Analysis of Single-Layer Networks in Unsupervised Feature Learning. *Journal of Machine Learning Research - Proceedings Track 15* (01 2011), 215–223.
- [13] Rodrigo F. de Mello, Yule Vaz, Carlos H. Grossi, and Albert Bifet. 2019. On learning guarantees to unsupervised concept drift detection on data streams. *Expert Systems with Applications* 117 (2019), 90–102. <https://doi.org/10.1016/j.eswa.2018.08.054>
- [14] Jacob Devlin, Ming-Wei Chang, Kenton Lee, and Kristina Toutanova. 2019. BERT: Pre-training of Deep Bidirectional Transformers for Language Understanding. In *Proceedings of the 2019 Conference of the North American Chapter of the Association for Computational Linguistics: Human Language Technologies, Volume 1 (Long and Short Papers)*. Association for Computational Linguistics, Minneapolis, Minnesota, 4171–4186. <https://doi.org/10.18653/v1/N19-1423>
- [15] Denis Moreira dos Reis, Peter Flach, Stan Matwin, and Gustavo Batista. 2016. Fast Unsupervised Online Drift Detection Using Incremental Kolmogorov-Smirnov Test. In *Proceedings of the 22nd ACM SIGKDD International Conference on Knowledge Discovery and Data Mining* (San Francisco, California, USA) (*KDD '16*). Association for Computing Machinery, New York, NY, USA, 1545–1554. <https://doi.org/10.1145/2939672.2939836>
- [16] Alexey Dosovitskiy, Lucas Beyer, Alexander Kolesnikov, Dirk Weissenborn, Xiuhua Zhai, Thomas Unterthiner, Mostafa Dehghani, Matthias Minderer, Georg Heigold, Sylvain Gelly, Jakob Uszkoreit, and Neil Houlsby. 2020. An Image is Worth 16x16 Words: Transformers for Image Recognition at Scale. *CoRR abs/2010.11929* (2020). <https://arxiv.org/abs/2010.11929>
- [17] D.C Dowson and B.V Landau. 1982. The Fréchet distance between multivariate normal distributions. *Journal of Multivariate Analysis* 12, 3 (1982), 450–455. [https://doi.org/10.1016/0047-259X\(82\)90077-X](https://doi.org/10.1016/0047-259X(82)90077-X)
- [18] Isvani Frías-Blanco, José del Campo-Ávila, Gonzalo Ramos-Jiménez, Rafael Morales-Bueno, Agustín Ortiz-Díaz, and Yailé Caballero-Mota. 2015. Online and Non-Parametric Drift Detection Methods Based on Hoeffding’s Bounds. *IEEE Transactions on Knowledge and Data Engineering* 27, 3 (2015), 810–823. <https://doi.org/10.1109/TKDE.2014.2345382>
- [19] João Gama and Gladys Castillo. 2006. Learning with Local Drift Detection. In *Advanced Data Mining and Applications*, Xue Li, Osmar R. Zaiane, and Zhanhui Li (Eds.). Springer Berlin Heidelberg, 42–55.
- [20] João Gama, Pedro Medas, Gladys Castillo, and Pedro Rodrigues. 2004. Learning with Drift Detection. In *Advances in Artificial Intelligence – SBIA 2004*, Ana L. C. Bazzan and Sofiane Labidi (Eds.). Berlin, Heidelberg, 286–295.
- [21] João Gama, Indrundefine Zliobaitundefined, Albert Bifet, Mykola Pechenizkiy, and Abdelhamid Bouchachia. 2014. A Survey on Concept Drift Adaptation. *ACM Comput. Surv.* 46, 4 (2014). <https://doi.org/10.1145/2523813>
- [22] Rosana Noronha Gemaque, Albert França Josuá Costa, Rafael Giusti, and Eulanda Miranda dos Santos. 2020. An overview of unsupervised drift detection methods. *WIREs Data Mining and Knowledge Discovery* 10, 6 (2020), e1381. <https://doi.org/10.1002/widm.1381>
- [23] Ömer Gözüağık, Alican Büyükcakır, Hamed Bonab, and Fazli Can. 2019. Unsupervised Concept Drift Detection with a Discriminative Classifier. In *Proceedings of the 28th ACM International Conference on Information and Knowledge Management* (Beijing, China) (*CIKM '19*). Association for Computing Machinery, New York, NY, USA, 2365–2368. <https://doi.org/10.1145/3357384.3358144>
- [24] Salvatore Greco and Tania Cerquitelli. 2021. Drift Lens: Real-time unsupervised Concept Drift detection by evaluating per-label embedding distributions. In *2021 International Conference on Data Mining Workshops (ICDMW)*. 341–349. <https://doi.org/10.1109/ICDMW53433.2021.00049>
- [25] Salvatore Greco, Bartolomeo Vacchetti, Daniele Apiletti, and Tania Cerquitelli. 2024. DriftLens: A Concept Drift Detection Tool. In *Proceedings 27th International Conference on Extending Database Technology, EDBT 2024, Paestum, Italy, March 25 - March 28*. OpenProceedings.org, 806–809. <https://doi.org/10.48786/edbt.2024.75>
- [26] Arthur Gretton, Karsten M. Borgwardt, Malte J. Rasch, Bernhard Schölkopf, and Alexander Smola. 2012. A Kernel Two-Sample Test. *Journal of Machine Learning Research* 13, 25 (2012), 723–773. <http://jmlr.org/papers/v13/gretton12a.html>
- [27] Philipp Grulich, René Saitenmacher, Jonas Traub, Sebastian Breß, Tilmann Rabl, and Volker Markl. 2018. Scalable Detection of Concept Drifts on Data Streams with Parallel Adaptive Windowing. <https://doi.org/10.5441/002/edbt.2018.51>
- [28] Ahsanul Haque, Latifur Khan, and Michael Baron. 2016. SAND: Semi-Supervised Adaptive Novel Class Detection and Classification over Data Stream. In *Proceedings of the Thirtieth AAAI Conference on Artificial Intelligence* (Phoenix, Arizona) (*AAAI'16*). AAAI Press, 1652–1658.
- [29] Martin Heusel, Hubert Ramsauer, Thomas Unterthiner, Bernhard Nessler, and Sepp Hochreiter. 2017. GANs Trained by a Two Time-Scale Update Rule Converge to a Local Nash Equilibrium, Vol. 30.
- [30] Shohei Hido, Tsuyoshi Idé, Hisashi Kashima, Harunobu Kubo, and Hirofumi Matsuzawa. 2008. Unsupervised Change Analysis Using Supervised Learning. In *Advances in Knowledge Discovery and Data Mining*, Takashi Washio, Einoshin Suzuki, Kai Ming Ting, and Akihiro Inokuchi (Eds.). Springer Berlin Heidelberg, Berlin, Heidelberg, 148–159.
- [31] Fabian Hinder, Valerie Vaquet, Johannes Brinkrolf, and Barbara Hammer. 2023. On the Hardness and Necessity of Supervised Concept Drift Detection. 164–175. <https://doi.org/10.5220/0011797500003411>
- [32] Fabian Hinder, Valerie Vaquet, and Barbara Hammer. 2023. One or Two Things We know about Concept Drift – A Survey on Monitoring Evolving Environments. arXiv:2310.15826 [cs.LG]
- [33] Hanqing Hu, Mehmed Kantardzic, and Tegjyot S. Sethi. 2020. No Free Lunch Theorem for concept drift detection in streaming data classification: A review. *WIREs Data Mining and Knowledge Discovery* 10, 2 (2020), e1327. <https://doi.org/10.1002/widm.1327>
- [34] Mikhail Hushchyn and Andrey Ustyuzhanin. 2020. Generalization of Change-Point Detection in Time Series Data Based on Direct Density Ratio Estimation. *CoRR abs/2001.06386* (2020). arXiv:2001.06386 <https://arxiv.org/abs/2001.06386>
- [35] Aditee Jadhav and Leena Deshpande. 2017. An Efficient Approach to Detect Concept Drifts in Data Streams. In *2017 IEEE 7th International Advance Computing Conference (IACC)*. 28–32. <https://doi.org/10.1109/IACC.2017.0021>

- [36] Daniel Kifer, Shai Ben-David, and Johannes Gehrke. 2004. Detecting change in data streams. In *Proceedings of the Thirtieth International Conference on Very Large Data Bases - Volume 30* (Toronto, Canada) (VLDB '04). VLDB Endowment, 180–191.
- [37] Young In Kim and Cheong Hee Park. 2016. Concept Drift Detection on Streaming Data under Limited Labeling. In *2016 IEEE International Conference on Computer and Information Technology (CIT)*. 273–280. <https://doi.org/10.1109/CIT.2016.34>
- [38] Anjin Liu, Yiliao Song, Guangquan Zhang, and Jie Lu. 2017. Regional Concept Drift Detection and Density Synchronized Drift Adaptation. 2280–2286. <https://doi.org/10.24963/ijcai.2017/317>
- [39] Anjin Liu, Guangquan Zhang, and Jie Lu. 2017. Fuzzy time windowing for gradual concept drift adaptation. In *2017 IEEE International Conference on Fuzzy Systems (FUZZ-IEEE)*. 1–6. <https://doi.org/10.1109/FUZZ-IEEE.2017.8015596>
- [40] Yinhan Liu, Myle Ott, Naman Goyal, Jingfei Du, Mandar Joshi, Danqi Chen, Omer Levy, Mike Lewis, Luke Zettlemoyer, and Veselin Stoyanov. 2019. RoBERTa: A Robustly Optimized BERT Pretraining Approach. *CoRR* abs/1907.11692 (2019). [arXiv:1907.11692](http://arxiv.org/abs/1907.11692) <http://arxiv.org/abs/1907.11692>
- [41] Jie Lu, Anjin Liu, Fan Dong, Feng Gu, João Gama, and Guangquan Zhang. 2019. Learning under Concept Drift: A Review. *IEEE Transactions on Knowledge and Data Engineering* 31, 12 (2019), 2346–2363. <https://doi.org/10.1109/TKDE.2018.2876857>
- [42] Edwin Lughofer, Eva Weigl, Wolfgang Heidl, Christian Eitzinger, and Thomas Radauer. 2015. Drift detection in data stream classification without fully labelled instances. In *2015 IEEE International Conference on Evolving and Adaptive Intelligent Systems (EAIS)*. 1–8. <https://doi.org/10.1109/EAIS.2015.7368802>
- [43] Mansour Zoubeirou A Mayaki and Michel Riveill. 2022. Autoregressive based Drift Detection Method. In *2022 International Joint Conference on Neural Networks (IJCNN)*. 1–8. <https://doi.org/10.1109/IJCNN55064.2022.9892066>
- [44] Tom Mitchell. 1999. Twenty Newsgroups. UCI Machine Learning Repository. DOI: <https://doi.org/10.24432/C5C323>
- [45] Kyosuke Nishida and Koichiro Yamauchi. 2007. Detecting Concept Drift Using Statistical Testing. In *Discovery Science*, Vincent Corruble, Masayuki Takeda, and Einoshin Suzuki (Eds.). Springer Berlin Heidelberg, 264–269.
- [46] Felipe Pinagé, Eulanda M. dos Santos, and João Gama. 2020. A Drift Detection Method Based on Dynamic Classifier Selection. *Data Min. Knowl. Discov.* 34, 1 (jan 2020), 50–74. <https://doi.org/10.1007/s10618-019-00656-w>
- [47] Eleonora Poeta, Gabriele Ciravegna, Eliana Pastor, Tania Cerquitelli, and Elena Baralis. 2023. Concept-based Explainable Artificial Intelligence: A Survey. [arXiv:2312.12936](https://arxiv.org/abs/2312.12936)
- [48] Stephan Rabanser, Stephan Günnemann, and Zachary Chase Lipton. 2018. Failing Loudly: An Empirical Study of Methods for Detecting Dataset Shift. In *Neural Information Processing Systems*. <https://api.semanticscholar.org/CorpusID:53096511>
- [49] Mohammad Rahimzadeh, Soroush Parvin, Elnaz Safi, and Mohammad Reza Mohammadi. 2021. Wise-SrNet: A Novel Architecture for Enhancing Image Classification by Learning Spatial Resolution of Feature Maps. *CoRR* abs/2104.12294 (2021). [arXiv:2104.12294](https://arxiv.org/abs/2104.12294) <https://arxiv.org/abs/2104.12294>
- [50] Victor Sanh, Lysandre Debut, Julien Chaumond, and Thomas Wolf. 2020. DistilBERT, a distilled version of BERT: smaller, faster, cheaper and lighter. [arXiv:1910.01108](https://arxiv.org/abs/1910.01108) [cs.CL]
- [51] Steffen Schneider, Alexei Baevski, Ronan Collobert, and Michael Auli. 2019. wav2vec: Unsupervised Pre-training for Speech Recognition. *CoRR* abs/1904.05862 (2019). [arXiv:1904.05862](https://arxiv.org/abs/1904.05862) <https://arxiv.org/abs/1904.05862>
- [52] Shreya Shankar and Aditya G. Parameswaran. 2022. Towards Observability for Production Machine Learning Pipelines. *Proc. VLDB Endow.* 15, 13 (sep 2022), 4015–4022. <https://doi.org/10.14778/3565838.3565853>
- [53] Pei Shen, Yongjie Ming, Hongpeng Li, Jingyu Gao, and Wanpeng Zhang. 2023. Unsupervised Concept Drift Detectors: A Survey. In *Advances in Natural Computation, Fuzzy Systems and Knowledge Discovery*. Springer International Publishing, Cham, 1117–1124.
- [54] Karen Simonyan and Andrew Zisserman. 2014. Very deep convolutional networks for large-scale image recognition. *arXiv preprint arXiv:1409.1556* (2014).
- [55] Nick Sun, Ke Tang, Zexuan Zhu, and Xin Yao. 2017. Concept Drift Adaptation by Exploiting Historical Knowledge. *IEEE Transactions on Neural Networks and Learning Systems* (2017). <https://doi.org/10.1109/TNNLS.2017.2775225>
- [56] Abhijit Suprem, Joy Arulraj, Calton Pu, and Joao Ferreira. 2020. ODIN: automated drift detection and recovery in video analytics. *Proc. VLDB Endow.* 13, 12 (jul 2020), 2453–2465. <https://doi.org/10.14778/3407790.3407837>
- [57] Arnaud Van Looveren, Janis Klaise, Giovanni Vacanti, Oliver Cobb, Ashley Sciliteo, Robert Samoilescu, and Alex Athorne. 2019. *Alibi Detect: Algorithms for outlier, adversarial and drift detection*. <https://github.com/SeldonIO/alibi-detect>
- [58] Francesco Ventura, Salvatore Greco, Daniele Apiletti, and Tania Cerquitelli. 2022. Trusting deep learning natural-language models via local and global explanations. *Knowledge and Information Systems* (2022). <https://doi.org/10.1007/s10115-022-01690-9>
- [59] Francesco Ventura, Salvatore Greco, Daniele Apiletti, and Tania Cerquitelli. 2023. Explaining deep convolutional models by measuring the influence of interpretable features in image classification. *Data Mining and Knowledge Discovery* (2023), 1–58.
- [60] Francesco Ventura, Stefano Proto, Daniele Apiletti, Tania Cerquitelli, Simone Panicucci, Elena Baralis, Enrico Macii, and Alberto Macii. 2019. A New Unsupervised Predictive-Model Self-Assessment Approach That SCALES. In *2019 IEEE International Congress on Big Data, Milan, Italy, July 8-13, 2019*. IEEE, 144–148. <https://doi.org/10.1109/BIGDATAACONGRESS.2019.00033>
- [61] P. Vorburger and A. Bernstein. 2006. Entropy-based Concept Shift Detection. In *Sixth International Conference on Data Mining (ICDM'06)*. <https://doi.org/10.1109/ICDM.2006.66>
- [62] Pingfan Wang, Hang Yu, Nanlin Jin, Duncan Davies, and Wai Lok Woo. 2024. QuadCDD: A Quadruple-based Approach for Understanding Concept Drift in Data Streams. *Expert Systems with Applications* 238 (2024), 122114. <https://doi.org/10.1016/j.eswa.2023.122114>
- [63] Xuezhi Wang, Haohan Wang, and Diyi Yang. 2022. Measure and Improve Robustness in NLP Models: A Survey. In *Proceedings of the 2022 Conference of the North American Chapter of the Association for Computational Linguistics: Human Language Technologies*. 4569–4586.
- [64] L. N. Wasserman. 1969. *Markov processes over denumerable products of spaces describing large systems of automata*. *Probl. Inform.*
- [65] Elias Werner, Nishant Kumar, Matthias Lieber, Sunna Torge, Stefan Gumhold, and Wolfgang E. Nagel. 2023. Examining Computational Performance of Unsupervised Concept Drift Detection: A Survey and Beyond. [arXiv:2304.08319](https://arxiv.org/abs/2304.08319) [cs.LG]
- [66] Shuliang Xu and Junhong Wang. 2017. Dynamic extreme learning machine for data stream classification. *Neurocomputing* 238 (2017), 433–449. <https://doi.org/10.1016/j.neucom.2016.12.078>
- [67] Kenji Yamaniishi and Jun-ichi Takeuchi. 2002. A unifying framework for detecting outliers and change points from non-stationary time series data. In *Proceedings of the Eighth ACM SIGKDD International Conference on Knowledge Discovery and Data Mining* (Edmonton, Alberta, Canada) (KDD '02). Association for Computing Machinery, New York, NY, USA, 676–681. <https://doi.org/10.1145/775047.775148>
- [68] Xiang Zhang, Junbo Jake Zhao, and Yann LeCun. 2015. Character-level Convolutional Networks for Text Classification. In *NIPS*.